Modeling of Dynamic Break in Underground Ring Blasting

Chris Preston, Troy Williams, Ian Lipchak

Abstract

Underground blasting operations are challenging from the standpoint of the distribution of explosives energy representative of ring blasting. Energy from both shock and pressure regimes of commercial explosives may appear concentrated in the collar region of a typical ring blast and diluted at the toes of holes due to the oblique geometries of blastholes. The non-homogenous nature of ore in which explosives are distributed via drillholes, adds to the complexities of generating particulate profiles from fragmented material with consistencies that are predictable from blast pattern to blast pattern - well suited for specific underground handling equipment and mill processing. In an ideal world, it would be the blasting operations themselves that represent the primary crushing mechanism, or at least mitigate mechanical crushing that can comprise a large component of the cost in generating suitable muck.

This paper presents a dynamic break view in 3D that allows a planner to visualize the potential break zone around a blasthole generated by an explosive load using a Kleine field. Simple as it sounds, this methodology provides information that can be used in conjunction with cavity monitoring surveys (CMS) to potentially judge dilution due to overbreak as well as recovery for a typical blast. As examples, there are two break geometries that are examined regarding circular breaks and elliptical breaks around blastholes. Using a Kleine field to define break, a planner generated isosurface can be generated and compared to CMS data for calibration and prediction, using AEGIS 3D ring design software.

Underground Blasting Operations

Powder factor limitations for underground blasting operations are listed with some observations;

- Patterns can be very complex and are constrained by the shape of the orebody as well as drift size and sublevel heights
- Perimeter control is used mostly in development operations and not generally used in stope blasting which may include Sublevel Cave (SLC), Open Stope Slot and Slash (OSS) as well as Vertical Retreat Mining (VRM)
- Mass blasts can be large and multilevel in scope – fragmentation is appraised as broken material is mucked out via scooptram
- Energy distribution from detonating explosives tends to be concentrated at the collar due to the confined nature of drilling from drifts and diluted at the toes because of the oblique geometry of rings
- Powder factors are not easily calculated and either estimated from toe to toe dimensions or calculated from the total volume of muck broken and the amount of explosives used
- Powder factors in many underground blasting operations appear to be twice those of surface blasting operations – break is hole to one-half the distance to an adjacent hole
- Free face for next row of drillholes (in a ring) is not visible; distance to next ring to detonate is not known
- The future of underground mining operations is to go deeper such that great attention is being focused on ground stability - especially with regard to blast design

There are severe constraints with regard to the design of underground blasting operations from the standpoint of ground support, ore block modeling - as well as production requirements that are dependent on the number of active workplaces. Safety is paramount. It becomes important to ensure that blasting

operations limit overbreak and dilution, including the restriction of overbreak into support structures. Recovery of valuable ore without dilution is the targeted goal of ring blasting design.

The Powder Factor Dilemma

In underground mining operations, the preference is to define PF (powder factor) as the weight of explosive required per unit volume or weight of ore used to fragment either a cubic meter or tonne of solid material. Thus, the units become kg/m^3 or kg/tonne using metric units, or lbs/yd^3 and lbs/ton in imperial units. Note that there is no direct association of ***explosive energy*** in the formula when powder factor is used as shown below:

$$\boldsymbol{PF = \frac{W_{Explosive}}{V_{ore}, W_{ore}}}\ ; \qquad (\mathbf{1})$$

Where:

$$\text{PF} = \text{powder factor}\ \left(\frac{kg}{m^3}; \frac{lbs}{yd^3}\right), \left(\frac{kg}{tonne}; \frac{lbs}{ton}\right)$$

$$\text{W}_{Explosive} = \text{weight of explosives used in blast (kg; lbs)}$$

$$V_{ore}, W_{Ore} = volume\ or\ weight\ of\ ore\ blasted\ (m^3, tonne;\ yd^3, ton)$$

Not being able to refer to energy in the formula causes problems not only from the oblique nature of ring design but also for predicting the degree of overbreak for individual stoping operations. It becomes quite apparent that blasthole geometry plays an extremely important role with regard to the focus of blast energy and how it will be distributed. The direction of blast motion becomes an important factor in insuring that blasting energy is propagated to the right free face (away from both topsill and bottomsill). PF is usually calculated on a per ring or per blast basis for a specific explosive type.

Different rock or ore types may require different weights of explosives to generate equivalent fragmentation profiles. If a low strength explosive is used, it may require blasting patterns to shrink in order to get the same fragmentation level as that produced by a higher strength explosive.

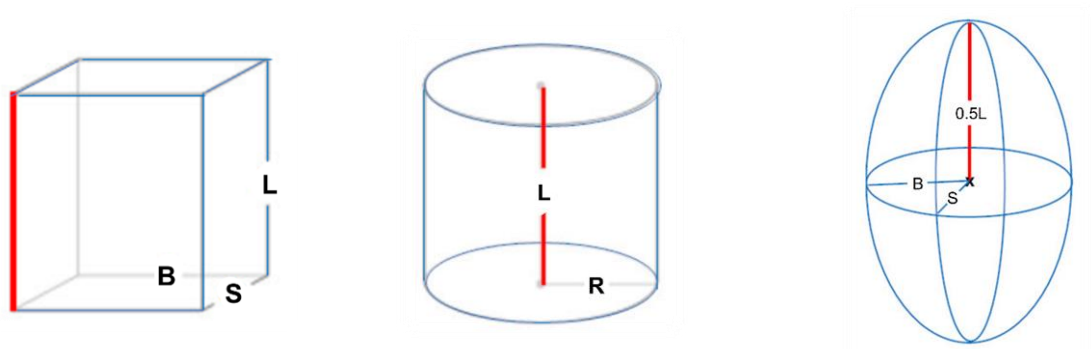

Rectangular Volume – 1(a)

$$\boldsymbol{V = BSL}\ ; \quad (\mathbf{2})$$

L = explosive column height
S = spacing
B = burden

Cylindrical Volume – 1(b)

$$\boldsymbol{V = \pi R^2 L}\ ; \quad (\mathbf{3})$$

L = explosive column height
R = radial break

Prolate Ellipsoid Volume – 1(c)

$$\boldsymbol{V = \frac{4}{3}\pi \times \frac{1}{2} L \times R^2}\ ; \quad \mathbf{(4)}$$

L = column height
B = burden, S = Burden, S = B = R

Figures 1(a), 1(b) and 1(c) illustrating some geometries to define powder factor.

The objective is to arrive at a calculation that is more likely to represent the action of a detonating explosive column in terms of geometrical 'break'- in which break represents the requisite number of crack pathways that provides a fragmentation profile required for mine handling equipment. Figure 1 attempts to rationalize rectangular volumes, which may be suitable for surface mining such that patterns are either square, rectangular and/or staggered, to geometric shapes that represent break action that is radially outward from a blasthole in a ring.

Underground mining operations demand drilling accuracy. Blastholes 100 mm (4 in) diameter are common for open stoping operations and can be long – sometimes over 5 times the length of blastholes drilled in open cast mining.

Drilling straight holes at the proper location can sometimes prove to be difficult. Figures 2(a), 2(b) and 2(c) below show the different types of errors that contribute to inaccuracies in blasting patterns responsible for distributing explosive energy throughout a rock/ore mass. In opencast mining operations, holes rarely exceed 20 m in depth.

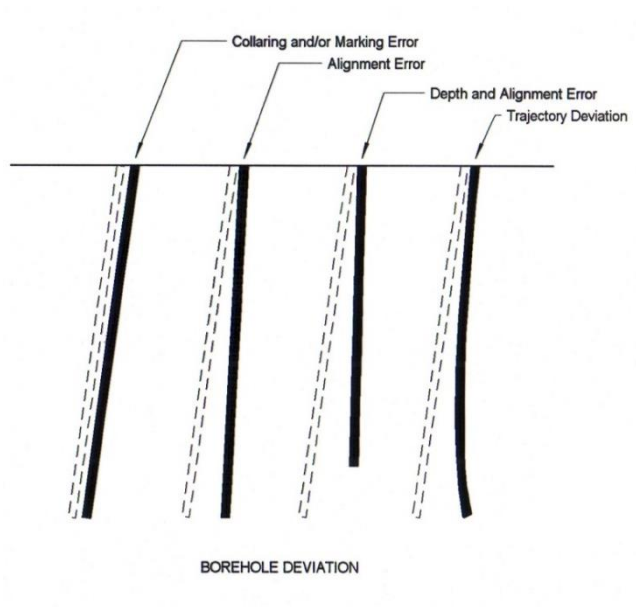

Figure 2(a)

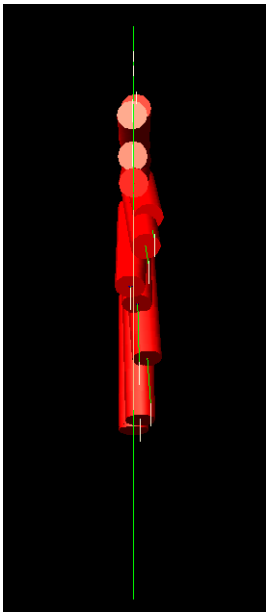

Figure 2(b)

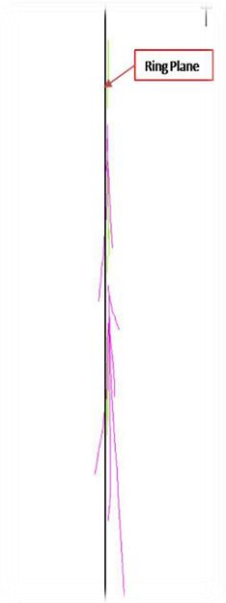

Figure 2(c)

Figure 2(a) illustrating typical drilling errors.
Figure 2(b) shows break cylinders that are in and out of the ring plane as shown in Figure 4.
Figure 2(c) indicates a ring longitudinal section (sideways view) in which holes are in and out of the ring plane seen in underground blasting operations.

For the case of underground PF's, ring geometries can be quite different and difficult to calculate.

Blastholes are not drilled to the same depth; the resulting geometry conforms to a quadrilateral forming a trapezium (a quadrilateral without parallel sides). Ring burden is used to calculate the volume addressed for each hole in a ring to define a representative PF .
To get an accurate powder factor, the total explosives used in an underground blast is divided by the total tons produced. This number can only be determined accurately when a stope has been completely mucked out.

Figure 3 shows some of the different quadrilateral shapes that can sometimes be used to calculate powder factor for rings.

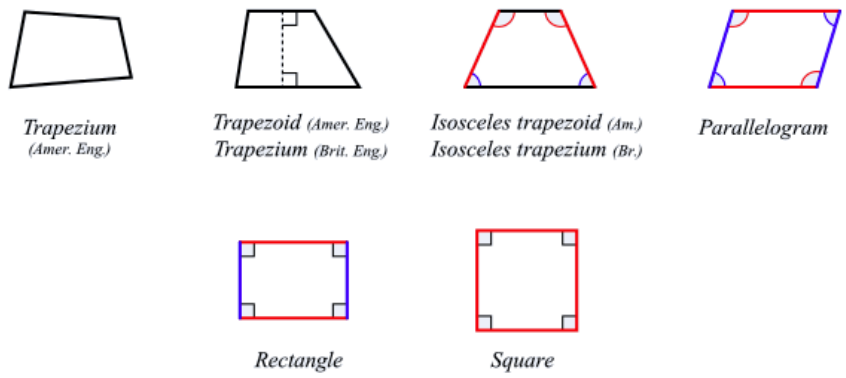

Figure 3 shows examples of four-sided shapes that may be used to calculate powder factor with the trapezium being very common for underground ring design.

Figures 4(a), 4(b) and 4(c) illustrate the trapezium type geometries that must addressed. Figure 4(c) is useful showing concentrations of energy and/or lack of it.

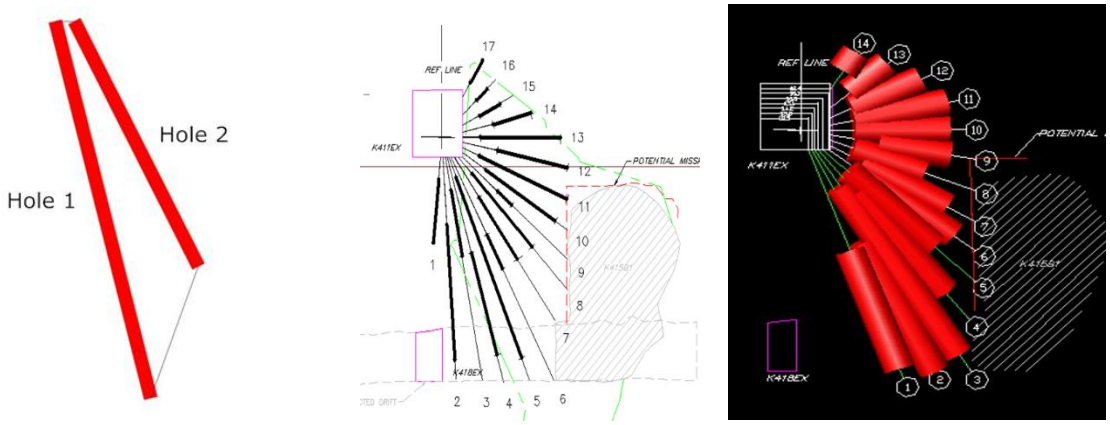

Figure 4(a) **Figure 4(b)** **Figure 4(c)**

Figure 4(a) shows a trapezium formed by connecting the collars and toes of two holes. The right angled distance between rings provides the burden component. Right angle distance between toes is assumed to provide the spacing component. Figure 4(b) illustrates a ring design in which the fragmentation suffers not only to drilling but also loading. In this case holes were not fully charged because of blocked holes with the belief that the next ring will take care of the drilling/loading problem.
Figure 4(c) shows an actual ring with 'break overlap' simulated for each hole defined by 'break' cylinders. Collars can be staggered to avoid concentration of energy in this region. In this view, it is easy to visualize the break around a blasthole based on a planner's experience.

For the cylindrical volume in which radial break is $R_{radial.cylinder}$, using Figure 1(b) for the Figure 8 cylindrical break example above, the formula for an equivalent radial break based on the volume calculation for an equivalent volume enclosed by a rectangular block (total confinement) is;

$$\boldsymbol{B \times S \times L = \pi \times R_{cylinder}{}^{2} \times L\,;} \quad \textbf{(5)}$$

$$\boldsymbol{R_{cylinder} = \sqrt{\frac{B \times S}{\pi}}\,; for\ cylindrical\ break\,;} \quad (\mathbf{6})$$

And, in a similar manner, the prolate ellipsoidal volume calculated such that B and S are equal and in the prolate case will represent the burden and spacing such that B^2 represents the break as shown below;

$$\boldsymbol{B \times S \times L = \frac{4}{3}\pi \times \frac{1}{2}L \times R_{ellipsoid}{}^{2}\,; for\ a\ prolate\ ellipsoid\,;} \quad (\mathbf{7})$$

$$\boldsymbol{R_{ellipsoid} = \sqrt{\frac{3 \times S}{2 \times \pi}}\,; for\ ellipsoidal\ break\,;} \quad (\mathbf{8})$$

By way of an example, using a ring pattern for sublevel cave mining with a toe spacing of 2.7 m (8.9 ft), with a 2.4 m (7.9 ft) burden between rings, and with the longest hole in the ring having a length of 30.5 m (100 ft). Using the rectilinear figure, the volume would be 198 m^3. With this volume as common to the other figures, the radial breaks can be approximated in Table 1. PF is based on a fully coupled emulsion explosive at a density of 1.25 gm/cm^3 in a 100 mm (4 in) borehole 30.5 m (100 ft) long.

Table 1 showing break dimensions in terms of common geometric shapes.

Geometrical Shape	Volume (m^3)	Radial Break (m)	Powder Factor (kg/tonne)
Rectangular $\boldsymbol{V = B \times S \times L}$	**198**		**1.51**
Cylindrical $\boldsymbol{V = \pi \times R_{cylinder}{}^{2} L}$		$\boldsymbol{R_{cylinder} = \sqrt{\frac{B \times S}{\pi}} = 1.44}$	
Prolate Ellipsoidal $\boldsymbol{V = \frac{4}{3}\pi \times \frac{1}{2}L \times B^2}$		$\boldsymbol{R_{ellipse} = \sqrt{\frac{3 \times S}{2 \times \pi}} = 1.77}$	

Using Internal Energy of a Commercial Explosive to Develop an Energy Factor

It becomes obvious that blasting patterns can be expanded using explosives that have higher densities of charge - even though the energy per unit of weight may be lower. The PF formula previously outlined contains no information concerning explosive energies. It is difficult to compare the PF for an ore type

using an ANFO or an emulsion based on PF alone with different energies as well as densities. Weight of ANFO cannot be compared to the same weight of emulsion, for example. It would be most convenient for explosive energy be brought into the calculation.

One of the problems using explosive internal energy is that commercial explosives are non-ideal meaning that detonation velocity increases gradually as the diameter of a charge increases. There is a critical velocity in which an explosive will detonate at a 'critical' diameter. This fact is usually noted in an explosive manufacturer's technical data sheet advising a user against loading an explosive in diameters below a critical one - along with a priming specification. The effect of varying detonation velocities, in specific diameters of charge, can be included in the energy (E_{exp}) calculation by taking into account the volumetric extent of reaction (N) which is represented by the following formula;

$$\boldsymbol{N = \left(\frac{VOD_{\emptyset}}{VOD_{ideal}}\right)^{2}} \; ; \qquad (\mathbf{9})$$

Where:

$$\boldsymbol{VOD_{\emptyset} = detonation\ velocity\ in\ charge\ diameter\ \emptyset}$$
$$\boldsymbol{VOD_{ideal} = ideal\ detonation\ velocity}$$

The density and energy values in the explosive datasheet are commonly given for the unreacted explosive. Hence, the bulk internal energy for unreacted explosive can be obtained from the above equation and can then be applied using the equation as indicated below;

$$\boldsymbol{E_{int} = \rho_{exp} \times E_{exp} \times \left(\frac{VOD_{\emptyset}}{VOD_{ideal}}\right)^{2} \times 0.239\,; \frac{MJ}{m^3}} \; ; \qquad (\mathbf{10})$$

Where:

$$\boldsymbol{E_{exp} = bulk\ internal\ energy\,; \frac{cal}{gm}}$$
$$\boldsymbol{\rho_{exp} = explosive\ density\,; \frac{gm}{cm^3}}$$

As an example, using the pattern dimensions from Table 1 in which spacing (S), burden (B) and the charge column length (L), a calculated volume of break (VOB_{break}) can be determined in Table 2 below;

Table 2 calculation parameters for volume of break for a rectilinear shape.

$\mathbf{S = 2.7\ m}$	$\mathbf{B = 2.4\ m}$	$\mathbf{L = 30.5\ m}$	$\mathbf{VOB_{break} = 198\ m^3}$

Assigning an explosive with the parameters below in Table 3, and using the above equation 10, the energy can be calculated for the loaded blasthole assuming that the VOD_{φ} = ¾ VOD_{ideal} as shown in Table 3;

Table 3 calculation parameters for determining $E_{internal}$ when VOD_{φ} = ¾ VOD_{ideal}

$\rho_{exp} = \mathbf{1.17\ \frac{gm}{cm^3}}$	$\mathbf{E_{exp} = 1000 \frac{cal}{gm}}$	$\mathbf{\emptyset = 0.100\ mm}$	$\mathbf{VOD_{\emptyset} = 4500 \frac{m}{s}}$	$\boldsymbol{VOD_{ideal} = 6000 \frac{m}{s}}$

Similarly, the energy determined for the ideal velocity case in which $VOD_{\varphi} = VOD_{ideal}$ is shown again in Table 4 using the parameters;

Table 4 calculation parameters for determining $E_{internal}$ when $VOD_{\varphi} = VOD_{ideal}$

$\rho_{exp} = 1.17\ \frac{gm}{cm^3}$	$E_{exp} = 1000\frac{cal}{gm}$	$\emptyset = 0.100$ mm	$VOD_{\emptyset} = 4500\frac{m}{s}$	$VOD_{ideal} = 6000\frac{m}{s}$

Table 5 presents break volume and break energy factor (EFbreak) of a single 100 mm blasthole example using an emulsion explosive such that VODφ is set to ¾VOD_{ideal} and VOD_{ideal}.

VOB_{break} (m^3)	ρ_{exp} (gm/cm^3)	E_{exp} (cal/gm)	$VOD_{\emptyset}$ (m/s)	VOD_{ideal} (m/s)	$E_{total.emulsion}$ (MJ/m^3)	$EF_{break.emulsion}$ (MJ)
198	1.17	1200	4500	6000	202	48
198	1.17	1200	6000	6000	359	86

The same analysis can be done using ANFO with the following properties and keeping the VOB_{break} the same – as indicated below and shown in Table 6.

Table 6 presents break volume and break energy factor (EFbreak) of a single 100 mm blasthole example using an ANFO explosive such that VODφ is being set to ¾VOD_{ideal} and VOD_{ideal}.

VOB_{break} (m^3)	ρ_{exp} (gm/cm^3)	E_{exp} (cal/gm)	$VOD_{\emptyset}$ (m/s)	VOD_{ideal} (m/s)	$E_{total.ANFO}$ (MJ/m^3)	$EF_{break.ANFO}$ (MJ)
198	0.85	880	3375	6000	101	24
198	0.85	880	4500	6000	178	43

Visualizing Break as a Production Estimation Tool for Underground Blasting Operations

Current blasting practices for underground blasting operations require drilling holes of a given diameter and with a very specific oblique geometry. This produces a drillhole pattern which is loaded with explosives and sequenced to generate a fragmentation profile that should be matched to materials handling equipment for a particular mining method. Many designs are obtained through trial and error based on historical results using a powder factor method. Software has been designed not only to mitigate the trial and error practice, but also to re-invent traditional methods of blast design in a very special way. The geometry of blast holes is oblique and irregular since holes are drilled from small confined spaces (drifts). In many cases there usually is a concentration of explosive energy in the collars with less energy at the toes of downholes (illustrated in Figures 4(b) and 4(c).

Using isosurfaces for radial break that a planner may estimate to visualize break are shown in Figure 5(a). Figure 5(b) represents an actual laser cavity scan (CMS–cavity monitoring survey) overlay including the planner's visualized break.

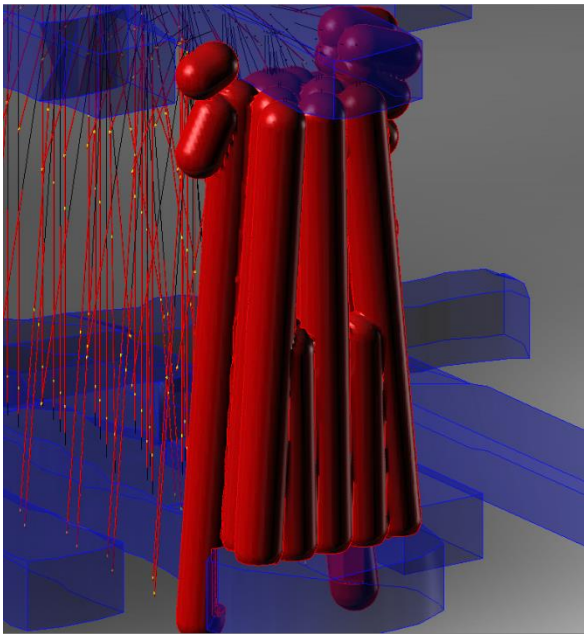

Figure 5(a)

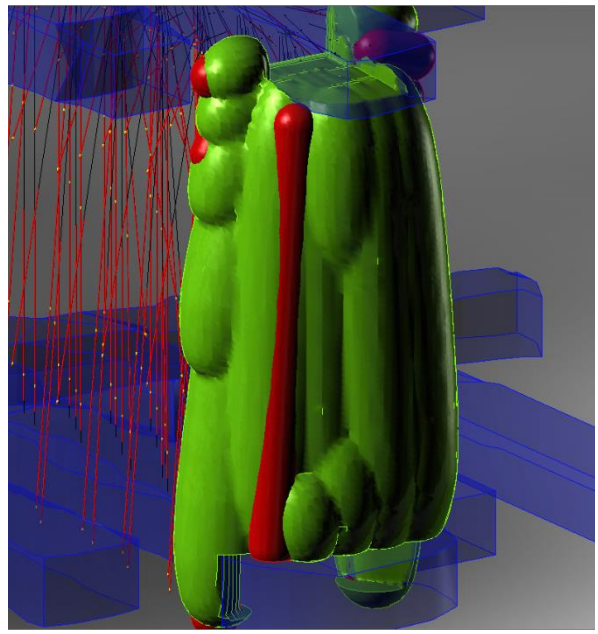

Figure 5(b)

Figure 5(a) shows a 1.5 m break isosurface for a 3 m × 3 m ring pattern.
Figure 5(b) places laser cavity scan (CMS-green) overlay on estimated planner break.

Using Break Based on a Kleine Field

It would be useful to generate a break field to determine whether or not there is excessive dilution resulting in poor recoveries as well as poor recoveries due to underbreak of a specific blast design. Using PF as a criteria, a Kleine break field can be generated to determine how closely a CMS fits.

A Kleine field is generated for a specific volume around the blast. This field is the basis of an isosurfacing mechanism in the 3D ring design software. A best fit function looks at the CMS and attempts to find an isosurface that best fits the CMS mesh. A symmetric difference approach is used between the CMS mesh and the Kleine isosurface. The isosurface that has the best percentage fit will be found after thousands of iterations.

For a Kleine field, it is convenient to consider a point source charge first, for any point *P* in proximity to a charge. If the point source fractures a spherical region of rock that ends at this arbitrary point, then the PF for that point source is simply the mass of the charge divided by the volume of the sphere. EF could be used as well – this work is in progress.

For a cylindrical source, the cylindrical charge can be divided up into a collection of point sources where each is treated as a point source and the 3D PF is defined as the sum of the contributions of all the point charges. For a charge of radius r_0, with an explosive density ρ_e, the 3D PF contribution of any charge segment of length *dx* is defined by.

$$\boldsymbol{PF_i(P) = \frac{1000 \cdot \rho_e \cdot \pi \cdot r_0^2 \cdot dx}{\frac{4}{3}\pi r^3}} \; ; \qquad (\mathbf{11})$$

Where r is the distance from point *P* to the charge segment. Defining the linear concentration of the charge (*q*) as the kg of explosive per meter of charge.

$$\boldsymbol{q = 1000\rho_e \cdot r_0} \; ; \qquad (\mathbf{12})$$

The above formula simplifies to:

$$\boldsymbol{PF_i(P) = \frac{q \cdot dx}{\frac{4}{3}\pi r^3}} \; ; \qquad (\mathbf{13})$$

The choice of the charge segment length is arbitrary, then let dx→0, and the sum of all the charge contributions can be expressed as an integral:

$$\boldsymbol{PF_i(P) = \int_0^l \frac{q \cdot dx}{\frac{4}{3}\pi r^3}} \; ; \qquad (\mathbf{14})$$

Then *l* is the length of the charge. The value r will be different for each point along the charge. Let Z be the linear offset of the point P from the toe of the charge, and R_0 is the distance from P to the line through the center of the charge. Figure 6 illustrates the geometry.

The unit vector $\boldsymbol{v}$ (direction of line through charge) and $\boldsymbol{u}$ (offset of *P* from the toe of the charge) make the computation of Z and R_0^2 fast and efficient in any orientation.

$$\mathbf{Z = u \cdot v} \;\; , \;\; \mathbf{R_0^2 = |u \cdot u - Z^2|} \; ; \qquad (\mathbf{15})$$

Kleine's model has an analytical solution as follows;

$$\boldsymbol{PF_i(P) = \frac{3q}{4R_0^2}\left(\frac{Z}{\sqrt{R_0^2 + Z^2}} - \frac{Z - l}{\sqrt{R_0^2 + (Z - l)^2}}\right)} \; ; \qquad (\mathbf{16})$$

The most desirable feature of Kleine's 3D powder factor field is it is defined as the sum of all the PF contributions of all charges within a blast. This means that where there are a number of charges in close proximity to each other and overlap, the 3D PF increases.

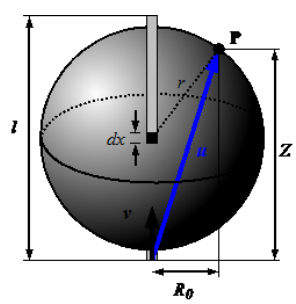

Figure 6 shows the geometry for a solution to a Kleine field.

Comparisons, Best Fit and Match Percent

For computing best-fit, the following definition applies. If an isosurface matches a CMS exactly, then a perfect fit is the result. Likewise, if there is no intersection between the 2 surfaces, then there is no perfect fit or a very poor one. In order to compare two meshes, both are converted to a voxel approximation. Essentially the meshes are reduced to small cubes, or voxels, approximating the mesh shapes. The size of voxels controls the accuracy of the approximation and comparison. The smaller the voxels, the more accurate. However there is a tradeoff - more voxels require more computational time. Boolean operations such as union and intersection can be unstable with meshes, whereas the voxels approximating the meshes have stable Boolean operations. Calculations consider the number of voxels where the 2 cavities do not agree divided by the number of voxels contained in either cavity. This is the volume of the symmetric difference divided by the volume of the union of the 2 cavities. This is shown in the following illustrations.

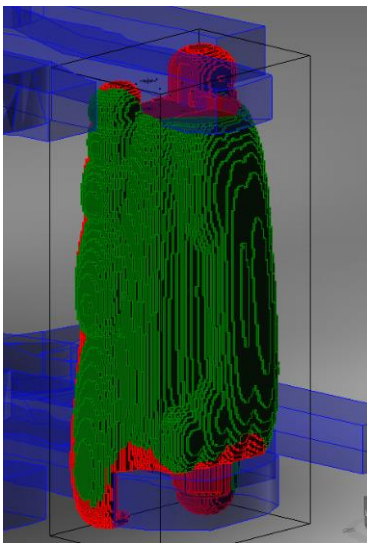

Figure 7(a)

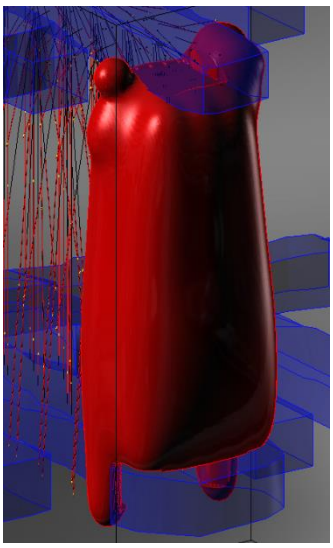

Figure 7(b)

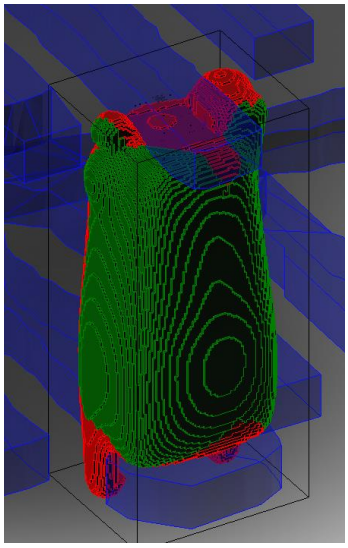

Figure 7(c)

Figure 7(a) represents the CMS from Figure 10 voxelized - using planner's break of 1.5 m.
Figure 7(b) illustrates the Kleine field overlay on a planner's estimated break of 1.5 m.
Figure 7(c) presents the Kleine field voxelized overlay on above break.

In Figure 7(a), the green blocks represent the part of the mesh that is in host rock. The red voxels represent the parts of the CMS that are in ore.

In Figure 7(c), this is the voxelized Kleine field from Figure 7(b) indicating which parts of the mesh are in ore (red) and which parts are in host rock (green)

As a comparison, the planner's estimated radial break can easily be increased to 2 m in order to give a CMS overlay for this new radial break to give the comparison below (comparison between Figure 5(a) and Figure 8(a).

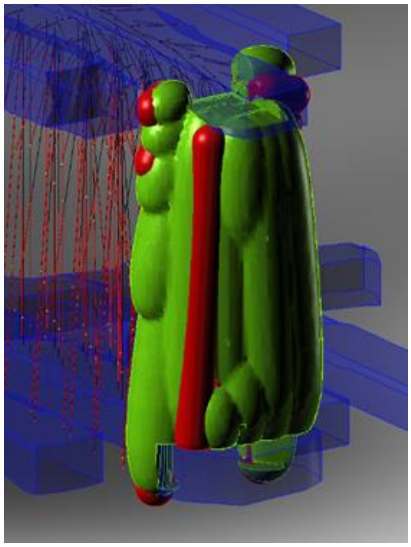

Figure 8(a)

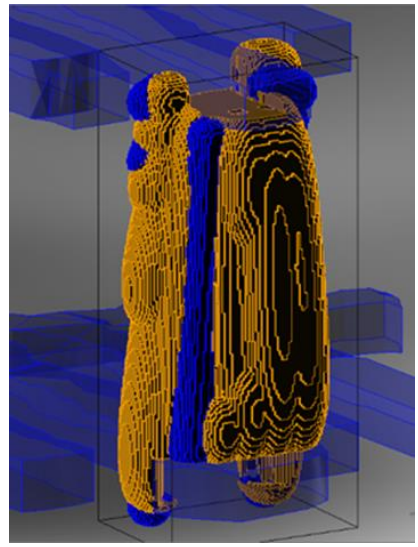

Figure 8(b)

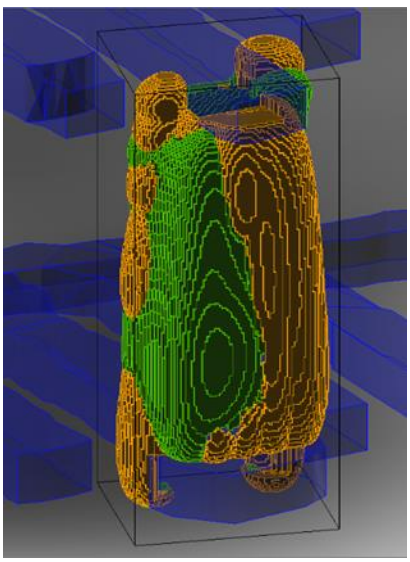

Figure 8(c)

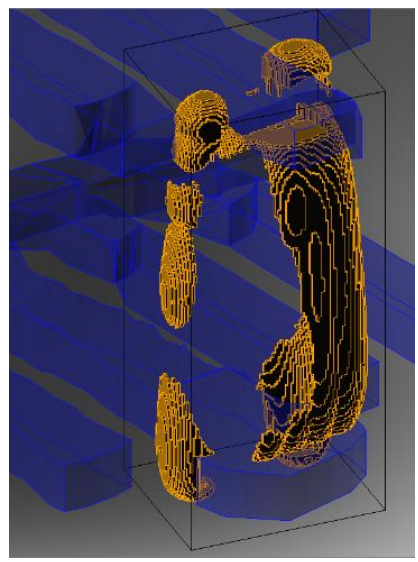

Figure 8(d)

Figure 8(a) represents the CMS overlay (green) on 2 m radial break (red).
Figure 8(b) shows the voxelized CMS overlay (gold) with voxelized break (blue).
Figure 8(c) represents the CMS overlay (gold) on the Kleine filed (green).
Figure 8(d) shows the voxelized CMS (gold). The Kleine field was subtracted leaving only the parts of the CMS that were not in common with the Kleine field.

Having tools that compare a planner's estimated break to a CMS along with using field predictions (such as the Kleine) are very valuable for optimizing blasting operations.

For example, a CMS can be used to calibrate the blast simulation model. The model can then be used to predict the final excavation break and, if the fragmentation characteristics of the various rock types are known, the predicted amount of fines and oversize as well. This would allow a blasting engineer to fine-tune the blast design for a best match of fragmentation to energy distribution and sequencing. Figure 9 shows the results for a typical simulation.

If this is continuously repeated blast by blast, the confidence in the model will increase as well as potentially give better prediction accuracy.

Property	Value
Name	Comparison 3
Prior Blast Voids Identical	True
Match %	62.83
Left Blast Total Volume (m³)	5,043.17
Left Blast Ore Volume (m³)	4,036.31
Left Blast Host Rock Volume (m³)	1,006.86
Right Blast Total Volume (m³)	7,552.28
Right Blast Ore Volume (m³)	5,074.22
Right Blast Host Rock Volume (m³)	2,478.06
Left Blast Total Tonnage (t)	14,930.77
Left Blast Ore Tonnage (t)	10,898.04
Left Blast Host Rock Tonnage (t)	4,032.72
Right Blast Total Tonnage (t)	23,625.65
Right Blast Ore Tonnage (t)	13,700.39
Right Blast Host Rock Tonnage (t)	9,925.26
Total Volume Difference (m³)	2,869.20

Figure 9 gives results of comparisons between a Klein field prediction and a CMS using a laser scan of a stope after ore has been completely mucked.

Note that the match was estimated to be roughly 63%. The additional data presented in the table contributes to the degree of precision of volumes required by the calculations to predict match percent. Additional simulations using the following procedure would gradually improve the match percent that is determined using the voxelization process for both the CMS survey and the Kleine Field;

1. After a production blast, a CMS data field from a laser scan is imported as a mesh into software,
2. Using the blast parameter information for interpolation of a Kleine field (either using PF or EF criteria) in order to generate a Kleine mesh based on blasthole layout and PF.
3. Determine the match percent using as voxelized CMS and Kleine field.
4. Change Kleine field parameters to obtain the best fit in order to guide the charging for the next blasting operation.

Recommendations for Future Work - Break Generation Using Crack Probability

A probability function may be able to be determined that represents 100% of the cracks passing through an elliptical shape (or any shape) close to the blasthole - with the probability falling off as the radial distance increases from the blasthole.

Work by other authors revised this idea using seismic tomography to get damage envelops and criteria with large charges. Such work proved that there was a minimum break fit of 100 percent passing through a well-defined shape (dependent of primer position) with a maximum break fit of less than 5 percent with increasing radial distances from a blasthole.

At some distance between these limits there is a blast pattern geometry that will generate a specific fragmentation required by loading and hauling equipment. The problem is to find that pattern based on probabilities of break using crack length distribution as a criteria as well as pattern geometry including primer position and delay sequencing.

It would be presumed that for a specific fragmentation the break probability based on crack length would be a defined number. This gets around trying to pin a precise number for a pattern dimension. It is a good way of working with geology from the standpoint of structure which would play a big role in influencing crack length probabilities.

The idea illustrated here is to show that at progressive radial distances out into a rock/ore mass the crack distribution might possibly be represented by a probability distribution. At a specific blasting pat-tern distance generating a fragmentation profile that fits an underground material handling system, there should be a distribution of cracks have a specific length that defines the distribution required based on the explosive properties, rock/ore properties and drilling layout. This preliminary model is shown in Figure 10.

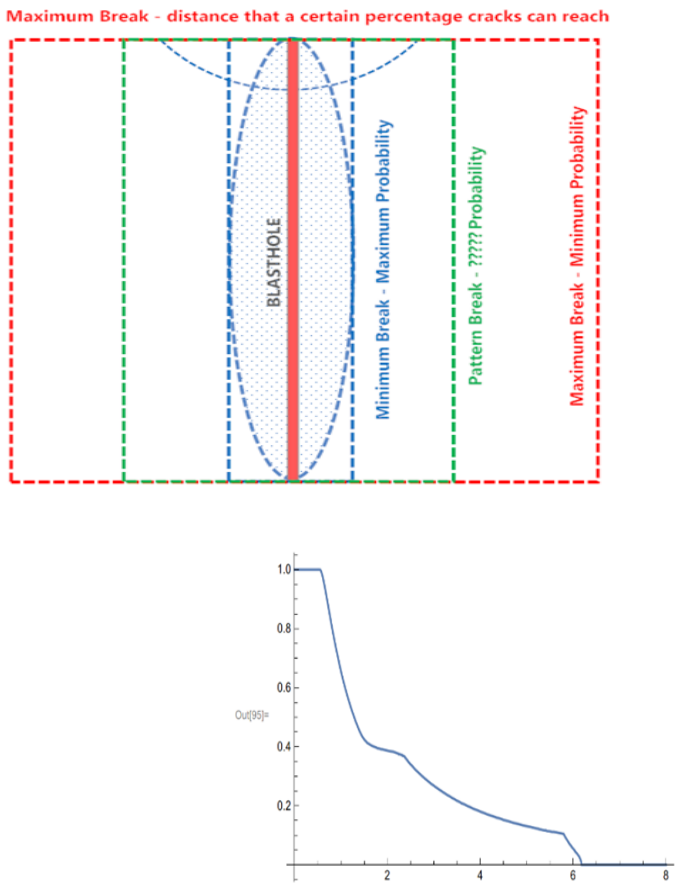

Figure 10 shows elliptical break (defined in Figure 1(c))in the top frame whereas the frame below represents the Y axis as percent probability, with the X axis being crack length in meters.

This model is presently undergoing data evaluation from testing completed at the Queen's University test site at Verona near Kingston, Ontario, Canada.

References

Alkins, Rob, IRAP Project, Analytic and Numerical Solutions to PPV Equations using 3D Co-ordinates. Report submitted for AEGIS IRAP Project 737345.

Kleine, T, 1988. A mathematical model of rock breakage by blasting. PhD Thesis. The University of Queensland, Australia. All pages.

Kleine, T, Cocker, A and Kavetsky, A, 1990. The development and implementation of a three dimensional model of blast fragmentation and damage. Proceedings of the third international symposium of rock fragmentation by blasting. The Australasian Institute of Mining and Metallurgy, Brisbane, Australia, Pages 181-187.

T.M. LeBlanc, J. M. Ryan & J. H. Heilig, Predicting the envelope of damage resulting from the detonation of a confined charge. Poster Session Pages 1-24.

Liu Q, Katsabanis P.D. A Theoretical Approach to the Stress Waves around a Borehole and their Effect on Rock Crushing. Fragblast 4, 1993. Complete Monogram

Onederra, I, 2001a. Development of an empirical fragmentation model for underground ring blasting applications. JKMRC/AMIRA Report, Submitted to BART II - P447 Project sponsors, August, Australia. Interim report.

Onederra, I, 2001b. Near Field Vibration Monitoring of SLC Ring blasting in XC11 of the 5305 level undercut. JKMRC-BARTII Project Report submitted to Newcrest Ridgeway, November.

Onederra, I, 2004 Breakage and fragmentation modelling for underground production blasting applications. IRR Drilling & Blasting 2004 Conference – Perth. Complete Monogram.

Onederra, I, 2004a. A fragmentation model for underground production blasting. PhD Thesis. The University of Queensland, Australia. Complete Monogram.

Onederra, I, 2004b. Modelling fragmentation in underground production blasting. Proceedings of the Massmin 2004 international conference, Santiago, Chile, 365-370.

Preston, C, 1995. 3D Blast design for ring blasting in underground mines. Proceedings of EXPLO 95 - The Australasian Institute of Mining and Metallurgy, Brisbane, Australia. Complete Monogram.

Preston C, Williams T. Results of Crack Propagation Tests in Granodiorite (Queen's University Test Site and Arnprior Limestone Quarry – MREL) - 2011 and 2012. NRC IRAP Project.

Ron J. Elliott, Chris Preston, and Daniel Roy, Use of In-situ Rock Properties for Optimization of Fragmentation, 12th Symposium on Explosives and Blasting Research, International Society of Explosives Engineers, 1996. Complete Monogram

Singh, S P, 1993. Prediction and Determination of Explosive Induced Damage. Rock Fragmentation by Blasting, Rossmanith (Ed.). Balkema, Rotterdam.

J. P. Tidman, Influence of Thermodynamics on the Calculation of Energies of Commercial Explosives, Explosives Research Laboratory, C-I-L Inc., McMasterville, Quebec, CANADA. Complete Monogram